



Estimating S-wave velocity of a coal seam excavation damaged zone in the vicinity of an underground coal mine roadway

V. Saineesh ¹, P. Sashikanth ²

V. Saineesh ¹ Asst. Prof. Dept of Mining Engineering, Malla Reddy Engineering College (Autonomous) Maisammaguda, Dhullapally post, via Kompally, Secunderabad-500100 India

P. Sashikanth ² Asst. Prof. Dept of Mining Engineering. Malla Reddy Engineering College (Autonomous) Maisammaguda. Dhullapally post, via Kompally, Secunderabad-500100 India

Abstract

We provide a new method for calculating the S-wave velocity of a fractured coal seam near an underground roadway. We use the so-called highway mode, which is a dispersive wave that propagates close to the sidewall of the road. We employ 3D finite-difference models to better comprehend the complicated seismic wavefield formed around the underground coal mine highway. The highway mode in the horizontal plane in the centre of the seam strives to the basic mode of the Rayleigh tunnel surface wave in the coal layer, according to modelling. As a result, the S-wave velocity model can be deduced from the dispersion curve of its group or phase velocity. The method's usefulness is proven using data from a 2-m thick coal seam. The sidewall mechanical quality is closely correlated with the derived quasi 2D S-wave velocity profile. For the damaged section of the road, we notice a drop in velocity. To increase safety and reduce economic loss while mining, the technology can be used to photograph and monitor fractured coal seams along a roadway in an underground coal mine.

Introduction

For the damaged section of the road, we notice a drop in velocity. To increase safety and reduce economic loss while mining, the technology can be used to photograph and monitor fractured coal seams along a roadway in an underground coal mine. Failure, increased support costs, and decreased mining safety can all result from a lack of detection and monitoring of its mechanical state. Its mechanical state is determined by P and S-wave velocities obtained using non-invasive seismic methods (eg., Barton, 2006). In tunnelling and underground mining, however, the gallery frequently runs parallel to horizontally stratified layers, each of which has distinct elastic properties. P-wave velocity from seismic refraction and S-wave velocity from surface waves approaches are difficult to acquire in such settings. Furthermore, when a low-velocity layer is surrounded by a high-velocity layer, such as surrounding a coal mine roadway, the wavefield becomes even more complicated



since guided waves exist (Essen et al., 2007; Czarny and Malinowski, 2020). As a result, obtaining the velocity profile of such a low-velocity layer is particularly difficult, and no reliable methods have been established for this purpose.

First, we look at the properties of seismic wavefields in a scenario that resembles an underground coal mine. We accomplish this by combining 3D finite-difference modelling with an analytical solution for dispersive waves. We show how to estimate S-wave velocity for a coal layer embedded in the EDZ based on our modelling results. Finally, we analyze data from a 2-m thick coal seam from the coal mine to offer real-world verification of our method.

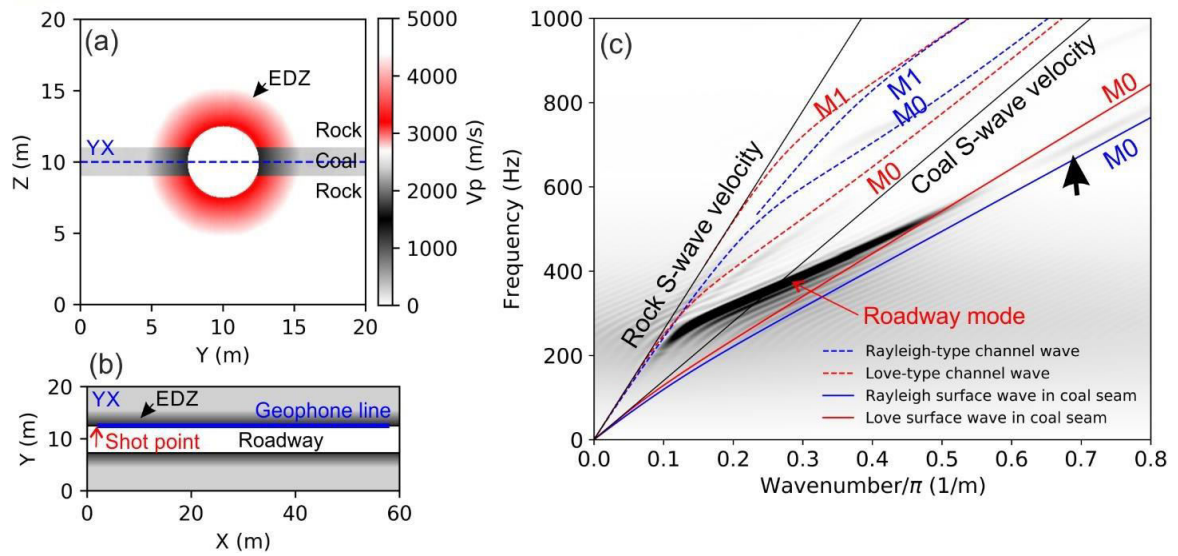
Theory and method

The presence of a highway sidewall, low-velocity coal seam inside the high-velocity host rock, and the EDZ are the key geophysical elements dictating seismic wave propagation characteristics in the region of an underground coal mine roadway. Together with the EDZ, the sidewall is a free-surface boundary that generates Rayleigh and Love tunnel surface waves. The rock-coal-rock structure, on the other hand, creates guided waves, often known as channel or seam waves (Krey, 1963). The results of 3D finite-difference simulations (Saenger and Bohlen, 2004) implemented in the SOFI3D open-source modelling system are shown in Figure 1. We put ourselves in the shoes of a regular underground coal miner. Table 1 contains the physical parameters.

Table 1: Finite-difference simulation parameters.

	Rock	Coal seam	Roadway
Thickness(m)		2	5
V_p (km/s)	04.5	2.4	0
V_s (km/s)	2.6	1.4	0.01
Density (g/cm^3)	2.6	1.4	1.25
Q_p	350	150	10e10
Q_s	140	60	10e10

At 3 m distant from the sidewall, we inject EDZ as a linear decrease of the parameters up to 30%. (Fig. 1a). We use a 0.05 m gap between gridpoints in the numerical model. We adjust the vacuum settings inside a circularly shaped roadway to represent a free-surface barrier. The source is positioned at the start of the model as a perpendicular force to the sidewall.



1st Figure (a) A P-wave velocity model with a cylindrically formed roadway and an EDZ is shown. (b) The position of the source point and the geophone line. (c) Theoretical dispersion curves for channel waves (red and blue dashed lines) and surface waves in the f-k domain for the horizontal component perpendicular to the roadway sidewall (red and blue solid lines). We mark this section of a highway mode with a black arrow, which propagates with a phase velocity similar to the Rayleigh tunnel surface wave (M0).

We utilise a sin wavelet with a centre frequency of 250 Hz. It has a significantly larger frequency band than the Ricker wavelet, therefore it can trace dispersive seismic waves much better.

The particle velocity is recorded by the geophone array at grid places on the walls (Fig. 1b). Figure 1c shows the particle velocity in the frequency-wavenumber (f-k) domain for the horizontal component perpendicular to the sidewall line. We also superimpose the analytical solutions for Rayleigh- and Love-type channel waves in a coal seam (Rader et al., 1985; Yang et al., 2014), as well as Rayleigh and Love tunnel surface waves for a coal seam with EDZ but no effect from surrounding rocks (Wathelet, 2008). A solid dispersive highway mode is observed (Lagasse and Mason, 1975; Krajewski et al., 1987; Czarny et al., 2020). This wave propagates with an S-wave velocity comparable to the host rock below 200 Hz and for a long wavelength. According to Jetschny et al. (2010), the free-surface boundary requirement can be ignored if the dispersive wave wavelength to roadway width ratio is greater than 1.6. The mid-wavelength highway mode is increasingly complex above 200 Hz, and its velocity is influenced by EDZ, coal, and host rock factors. Finally, the highway mode aspires to the basic mode of a Rayleigh tunnel surface wave for a short wavelength (Fig. 1, black arrow). We must estimate numerous unknown parameters (velocities, densities, EDZ thicknesses, coal seam thicknesses, and hosted rocks) from only one curve in order to invert the highway mode dispersion curve to S-wave velocity, making it very non-unique. However, we can compute the S-wave velocity model for short wavelengths by treating the

highway mode as a foundation mode of the Rayleigh tunnel surface wave. It's worth mentioning that the smaller the EDZ that can be photographed, the thinner the coal seam. In general, the wavelength should not be longer than the thickness of the coal seam.

Example

We use inferences from the modelling part to invert Rayleigh tunnel surface wave group velocity dispersion curves to S-wave velocity models in an underground experiment at coal mine. It enables us to visualize the EDZ's farthest reaches within the coal seam. The section of the road with noticeable changes in the sidewall's mechanical status is chosen. In this manner, we set up 12 horizontal geophones along with the seismic profile, half of which were installed on high-quality sidewalls (Fig. 2., geophones 1-6). The rest (geophones 7-12 in Fig. 2) are mounted on the damaged sidewall. The geophone's native frequency is 10 Hz.

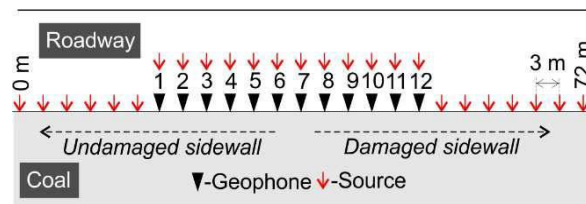


Figure2. Geometry of the underground experiment. The first six geophones were installed in the undamaged part of the sidewall and there the damaged part of the sidewall.



The distance between them is 3 metres. The geophones are mounted on 30 cm steel rods fastened to the walls in the seam's middle. Figure 3 depicts an example of recorded traces sorted in a common-offset gather for a 12 m offset. That offset was chosen for two reasons. First, we wish to investigate highway mode in higher frequency ranges, which necessitates an emphasis on short offset owing to attenuation. Second, where the highway mode does not fully emerge, the offset must be too short to be influenced by the near-field effect for dispersive waves (Foti et al., 2014). (Czarny and Malinowski, 2020). The reciprocity concept is used to stack the traces for equal ray routes. Along the profile, we notice changes in the waveforms. The early arrival times are substantially faster than the latter ones for raw data (Fig. 3a) up to roughly 36 m. It implies that seismic waves have higher velocities for the undamaged portion of the sidewalls in general. The frequencies for the traces at the start of the profile are likewise noticeably higher (shorter distances between following peaks and thorough). The reason for this is that the undamaged area of the sidewall has weaker attenuation. We show high-pass filtered signals above 380 Hz in Figure 3b. Each trace is made up of a dispersed bundle of seismic waves, as can be seen. We see a drop in group velocity towards the end of the seismic profile, similar to raw data.

Inversion

Higher frequencies of the highway mode recorded in the middle of the seam by the component perpendicular to the sidewall by the component perpendicular to the sidewall comprise mostly the fundamental mode of the Rayleigh tunnel surface wave, as indicated by our modelling. As a result, we examine our high-pass filtered common-offset traces in the frequency – group velocity domain to find Rayleigh surface wave basic mode dispersion curves. Figure 4 shows an example of typical frequency-time analysis (Dziewoski et al., 1969) for a trace with a mid-point of 15 m. The core energy packet's dispersed form is obvious. For each tracing, we display selected dispersion curves in Figure 5. For the first 30 metres of the undisturbed walls, we notice increased frequencies and group velocities. We select curves for wavelengths less than 2 m in general. Prior to inversion, we create an initial model with linear velocity increases that are similar to those found in modelling. With velocities fixed between 400 and 1500 m/s, the first model finishes at a depth of 2 m. In the inversion, we employ the neighborhood algorithm (Sambridge, 1999), which is implemented in Geopsy software (Wathelet, 2008). We end up with 16 1D S-wave velocity models. The RMS misfit errors between the measured and computed dispersion curves are less than 7%. The inversion procedure's results are shown in Figure 6. In general, we can image up to 1.3 m inside the EDZ for a 2 m coal seam thickness. The speed varies between 150 and 820 m/s. The undamaged portion of the route has the highest velocities. In general, we see a drop in velocity as we approach the damaged section of the road.

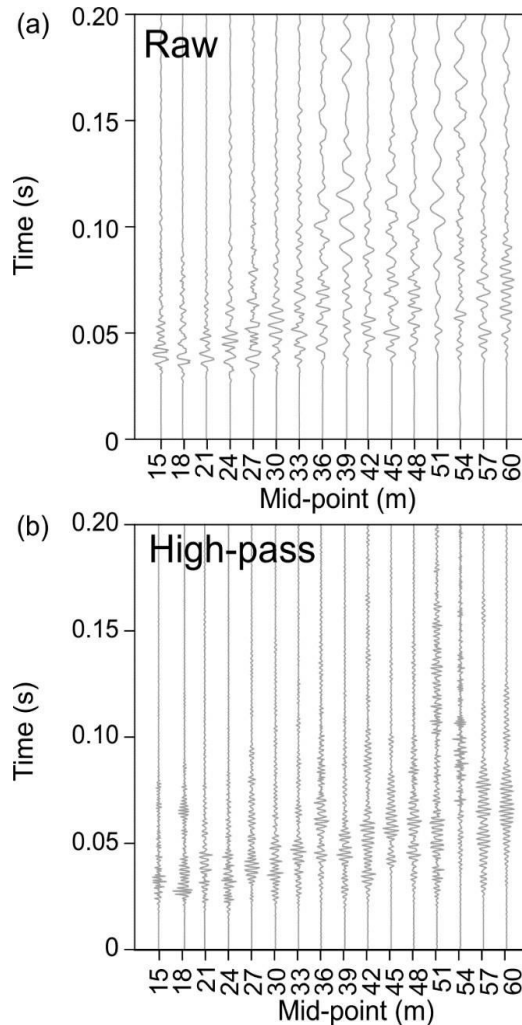


Figure3. The common-off set gathers for off set equal 12m.
(a) Raw traces and (b) high-pass filtered traces above 380Hz.

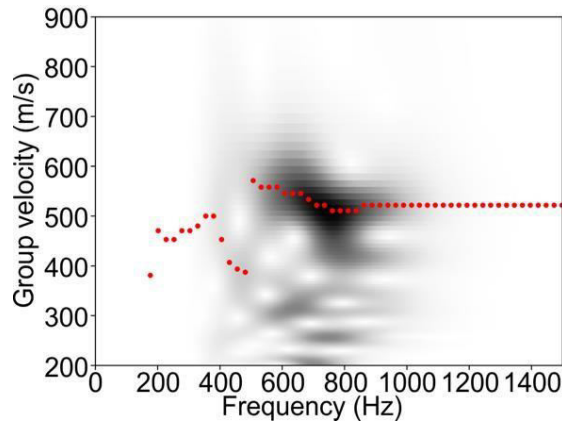


Figure4. An example of the roadway mode in frequency-velocity domain.

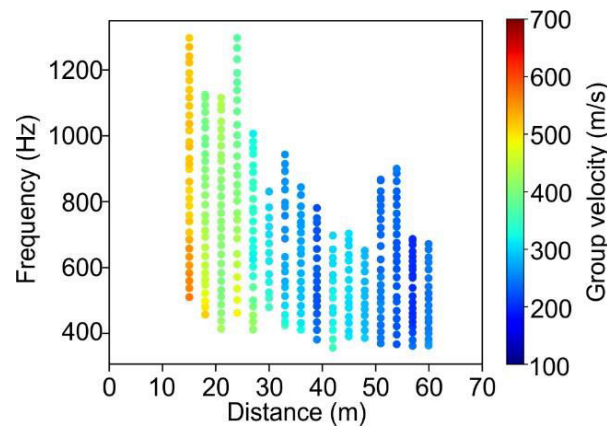


Figure5. Group velocity dispersion curves of fundamental mode of Rayleigh tunnel surface wave.

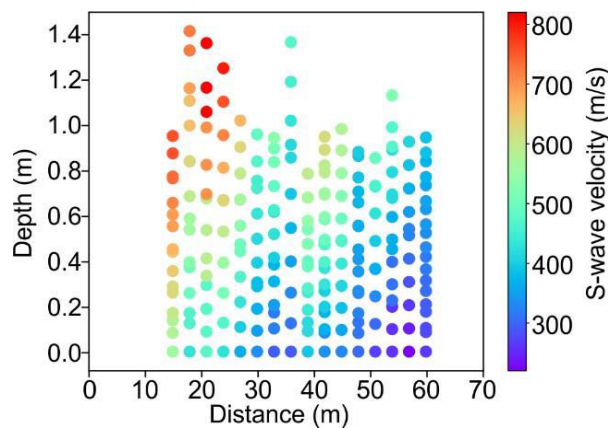


Figure6. S-wave velocity changes along the profile inverted from group velocity dispersion curves of fundamental mode of Rayleigh tunnel surface wave.



Conclusions

The excavation damaged zone in the coal seam along the underground coal mine roadway is imaged using S-wave velocity imaging. The mechanical state of the sidewall is correlated with the estimated S-wave velocity models. The leading energy of a highway mode within the EDZ for higher frequencies in the horizontal plane in the middle of the seam travels as a fundamental mode of the Rayleigh tunnel surface wave, according to our method, which is based on numerical simulations. As a result, the S-wave velocity model can be inverted. The fundamental disadvantage of this method is that the imaging range is limited by the thickness of the coal seam. In general, the thicker the coal seam, the deeper the penetration. Furthermore, the proposed method was evaluated on a coal seam with no additional disturbances such as faults or dirt bands. Estimating S-wave velocity from the entire highway mode record, particularly for low- and high-velocity layers, is still a work in progress.

REFERENCES

- Barton, N., 2006, Rock quality, seismic velocity, attenuation and anisotropy: CRC Press, doi: <https://doi.org/doi:10.1201/9780203964453>.
- Czarny, R., and M. Malinowski, 2020, Modeling of seismic wave propagation around coal mine roadway with presence of excavation-damaged zone: EGU General Assembly Conference Abstracts, 4797, doi: <https://doi.org/10.5194/egusphere-egu2020-4797>.
- Czarny, R., M. Malinowski, M. Cwiekala, S. Olechowski, Z. Isakow, and P. Sierodzki, 2020, Characterisation of the tunnel-channel wave around a coal mine roadway based on synthetic and real data: NSG2020 3rd Conference on Geophysics for Mineral Exploration and Mining, European Association of Geoscientists & Engineers, 1–5, doi: <https://doi.org/10.3997/2214-4609.202020024>.
- Dziewonski, A., S. Bloch, and M. Landisman, 1969, A technique for the analysis of transient seismic signals: Bulletin of the Seismological Society of America, 59, 427–444, doi: <https://doi.org/10.1785/BSSA0590010427>.
- Essen, K., T. Bohlen, W. Friederich, and T. Meier, 2007, Modelling of Rayleigh-type seam waves in disturbed coal seams and around a coal mine roadway: Geophysical Journal International, 170, 511–526, doi: <https://doi.org/10.1111/j.1365-246X.2007.03436.x>.
- Foti, S., C.G. Lai, G.J. Rix, and C. Strobbia, 2014, Surface wave methods for near-surface site characterization: CRC Press, doi: <https://doi.org/10.1201/b17268>.
- Jetschny, S., T. Bohlen, and D. De Nil, 2010, On the propagation characteristics of tunnel



- surface-wavesforseismicprediction:Geophysical Prospecting,58,245–256,doi:<https://doi.org/10.1111/j.1365-2478.2009.00823.x>.
- Krajewski, P., L. Dresen, W. Schott, and H. Ruter, 1987, Studies of roadway modes in a coal seam by dispersion and polarization analysis: A casehistory:GeophysicalProspecting,35,767–786,doi:<https://doi.org/10.1111/j.1365-2478.1987.tb02257.x>.
- Krey, T., 1963, Channelwavesasatoolofappliedgeophysicsincoalmining:Geophysics,28,no.5,701–714,doi:<https://doi.org/10.1190/1.1439258>.
- Lagasse, P. E., and I. M. Mason, 1975, Guided modes in coal seams and their application to underground seismic surveying: Ultrasonics SymposiumProceedingsIEEECat.75CHO994-4SU,64–67,doi:<https://doi.org/10.1109/ULTSYM.1975.196466>.
- Leparoux, D., P. Côte, C. Gélis, and J.Cabrera-Nunez, 2012, EDZ characterizationwith surface waveanalysis: An experimental and numerical studyfor defining feasibility in the context of the Tournemire platform (France): Near Surface Geophysics, 10, 401–411, doi: <https://doi.org/10.3997/1873-0604.2012033>.
- Rader, D., W. Schott, and H. Ruter, 1985, Calculation of dispersion curves and amplitude-depth distributions of love channel waves in horizontal-layeredmedia.GeophysicalProspecting,33,800–816,doi:<https://doi.org/10.1111/j.1365-2478.1985.tb00779.x>.
- Sambridge, M., 1999, Geophysical inversion with a neighbourhood algorithm -I. Searching a parameterspace: Geophysical Journal International, 138,479–494,doi:<https://doi.org/10.1046/j.1365-246X.1999.00876.x>.
- Saenger, E.H., and T.Bohlen,2004, Finitedifference modelingof viscoelasticand anisotropicwave propagationusingtherotatedstaggeredgrid:Geophysics,69,no.2,583–591,doi:<https://doi.org/10.1190/1.1707078>.
- Wang, H., Y. Jiang, S. Xue, B. Shen, C. Wang, J. Lv, and T. Yang, 2015, Assessmentofexcavationdamag edzonearoundroadwaysunderdynamicpressureinducedbyanactiveminingprocess:InternationalJournalofRockMechanicsandMiningSciences,77,265–277,doi:<https://doi.org/10.1016/j.ijrmms.2015.03.032>.
- Wathelet, M., 2008, An improved neighborhood algorithm: parameter conditions and dynamic scaling: Geophysical Research Letters, 35, L09301, doi: <https://doi.org/10.1029/2008GL033256>.
- Yang, X.H., S.Y. Cao, D.C. Li, P.F. Yu, and H.R. Zhang, 2014, Analysis of quality factors for Rayleigh channel waves: Applied Geophysics, 11, 107–114, doi: <https://doi.org/10.1007/s11770-014-0409-5>.